Available online at www.sciencedirect.com
SCIENCE DIRECT®
Polymer 45 (2004) 3399–3412
polymer
www.elsevier.com/locate/polymer

Absorption of CO_2 and subsequent viscosity reduction of an acrylonitrile copolymer

Michael J. Bortner, Donald G. Baird*

Department of Chemical Engineering and Center for Composite Materials and Structures, Virginia Polytechnic Institute and State University, 128 Randolph Hall, Blacksburg, VA 24061-0211, USA

Received 26 February 2004; accepted 3 March 2004

Abstract

Acrylonitrile (AN) copolymers (AN content greater than about 85 mol%) are traditionally solution processed to avoid a cyclization and crosslinking reaction that takes place at temperatures where melt processing would be feasible. It is well known that carbon dioxide (CO_2) reduces the glass transition temperature (T_g) and consequently the viscosity of many glassy and some semi-crystalline thermoplastics. However, the ability of CO_2 to act as a processing aid and permit processing of thermally unstable polymers at temperatures below the onset of thermal degradation has not been explored. This study concentrates on the ability to plasticize an AN copolymer with CO_2, which may ultimately permit melt processing at reduced temperatures. To facilitate viscosity measurements and maximize the CO_2 absorption, a relatively thermally stable, commercially produced AN copolymer containing 65 mol% AN was investigated in this research. Differential scanning calorimetry (DSC) and thermogravimetric analysis (TGA) indicated that CO_2 significantly absorbs into and reduces the T_g of the AN copolymer. Pressurized capillary rheometry indicated that the magnitude of the viscosity reduction is dependent on the amount of absorbed CO_2, which correlates directly to the T_g reduction of the plasticized material. Up to a 60% viscosity reduction was obtained over the range of shear rates tested for the plasticized copolymer containing up to 6.7 wt% CO_2 (31 °C T_g reduction), corresponding to as much as a 30 °C equivalent reduction in processing temperature. A Williams–Landel–Ferry (WLF) analysis was used to estimate the viscosity reduction based on the T_g reduction (and corresponding amount of absorbed CO_2) in the plasticized AN copolymer, and the predicted viscosity reduction based on using the universal constants was 34–85% higher than measured, depending on the amount of absorbed CO_2. Van Krevelen's empirical solubility relationships were used to calculate the expected absorbance levels of CO_2, and found to be highly dependent on the choice of constants within the statistical ranges of error of the Van Krevelen relationships.

Keywords: Carbon dioxide; Acrylonitrile; Plasticizer

1. Introduction

Because of the thermally unstable nature of acrylonitrile (AN) copolymers, generally containing about 85 mol% or greater AN when no stabilizer is present [1], they are processed in the presence of toxic, organic solvents, commonly including dimethlyl formamide (DMF) and dimethylacetamide (DMAC). Viscosities for these materials generally become suitable for melt processing when temperatures of approximately 220 °C are approached [1]. However, at 220 °C a rapid reaction that produces intramolecular cyclic structures with intermolecular crosslinks takes place, rendering these high AN content copolymers intractable prior to extrusion into fiber form [2]. The crosslinking reaction can be slowed by the presence of a stabilizer, such as boric acid, particularly for relatively low molecular weight AN copolymers containing between 85–90 mol% AN [3]. Acrylic fibers from high molecular weight AN precursors, especially containing greater than 90 mol% AN, are typically solution processed at low solids content (7–30 wt% polymer) using toxic organic solvents [4].

The need exists for a less expensive and environmentally benign process (compared to solution spinning in toxic organic solvents) for producing AN copolymer fibers suitable for use as carbon fiber precursors and textiles [5]. The melt processing of AN copolymers could potentially provide a solution to both of these issues by increasing solids throughput on a per pound basis and eliminating the need for solvent use and recovery [1]. In order to melt

* Corresponding author. Tel.: +1-540-231-5998; fax: +1-540-231-5022.
E-mail address: dbaird@vt.edu (D.G. Baird).

0032-3861/$ - see front matter © 2004 Elsevier Ltd. All rights reserved.
doi:10.1016/j.polymer.2004.03.021

process AN copolymers, the kinetics of the crosslinking reaction described above need to be kept to a minimum. Bhanu and co-workers [6] have shown that the crosslinking kinetics for copolymers with AN molar ratios of 85–90% become significant when a temperature on the order of 220 °C was reached. However, the viscosity level was suitable for melt processing these materials at this temperature. The same AN copolymers were shown by Rangarajan and co-workers [1,7] to possess a stable steady shear viscosity over a 30 min test period when the test temperature was reduced by 20–200 °C, indicative of a significant reduction in the kinetics of the crosslinking reaction, but the viscosity was too high for extrusion operations. These results suggest that reducing the processing temperature of AN copolymers by 20 °C could sufficiently reduce the kinetics of the crosslinking reaction in high AN content copolymers, permitting melt processing without significant degradation, assuming a viscosity suitable for melt extrusion can be obtained.

Numerous patents and journal articles have been published regarding melt processing of polyacrylonitrile copolymers using a plasticizer [5,8–16]. The majority of studies focused on the use of water to plasticize an AN homopolymer (or copolymer) for melt extrusion. Coxe [8] showed that water plasticizes AN copolymers and permits melt processing at reduced temperatures, but Porosoff [13] showed that the extrudate needed to be passed through a pressurized solidification zone to prevent foaming of the fiber. Studies have shown that the removal of water from the precursor fiber is quite difficult, and as a result the stabilized and carbonized fibers could not be produced without formation of a microporous structure at the fiber core [5, 16]. To permit removal of the water from the fibers, a process was developed combining acetonitrile, methanol, and water to plasticize AN copolymers and melt process them into carbon fibers [10,11]. The addition of acetonitrile and methanol lowered the boiling point of the water and facilitated its removal from the fibers. However, approximately 25–45 wt% plasticizer was necessary for processing, and it still required recovery because of the hazardous nature of acetonitrile, which degrades into cyanide at relatively low temperatures. As a result, the process provided no economic benefit over the solution process once commercial production outputs (greater than 2×10^6 lb per year) were reached.

Potentially melt processable AN copolymers have also been investigated by Bhanu et al. [3,6] and Rangarajan et al. [1,7]. The studies focused on the use of suitable comonomers (primarily MA) in the range of 10–15 mol% to disrupt the long range order and reduce the T_g of AN copolymers, rendering them melt stable. Kinetics of crosslinking were found to be very slow in the melt stable AN copolymers, which presented a problem when attempting thermo-oxidative stabilization (part of the carbonization process) of the resultant fibers [3]. As a result, a third comonomer (acryloyl benzopenone) was copolymerized to initiate the crosslinking reaction via UV irradiation following fiber formation [3]. The terpolymers could be melt processed into fibers with minimal degradation, but it was found that the kinetics of crosslinking became too rapid for melt processing if acrylonitrile contents greater than about 85 mol% were used.

Concern over volatile organic solvent emissions and contamination has also initiated searches to find cleaner solvents for both polymer synthesis and polymer processing [17]. Liquid and supercritical carbon dioxide (Sc-CO_2) have been a recent focal point for organic solvent replacement [18]. The benefits of using CO_2 over typical organic solvents are numerous. Carbon dioxide is non-toxic, non-flammable, environmentally friendly, recoverable, and supercritical conditions ($T_c = 31.1$ °C, $P_c = 7.39$ MPa) are easily reached. In the supercritical state, CO_2 is known to have similar solubilization characteristics to organic solvents (such as hexane) and CFC's. Sc-CO_2 also possesses a diffusivity similar to that of a gas, but a density like that of a liquid, which promotes rapid plasticization in amorphous materials [19]. For these and many more reasons, Sc-CO_2 has proven to be a very versatile alternative in some solvent based applications and consequently has been the focus for a surge of interest in many commercial applications [17], including ceramics processing, paper deacidification, metal cleaning, and plastics and textiles processing [18].

There have only been a few studies reported which have focused on the ability to plasticize thermoplastics with CO_2 and the subsequent effect on the viscosity. The interactions of various amorphous and semi-crystalline polymers with CO_2 have been studied and documented [20,21]. Semi-crystalline polymers, in general, have been shown to absorb CO_2 and be plasticized to a lesser extent than amorphous polymers [21]. Also, polarity has been shown to play a crucial role in CO_2 absorption, with higher polarity increasing the solubility in amorphous polymers [20]. CO_2 has been shown to plasticize a significant number of thermoplastics, including polydimethylsiloxane (PDMS) [22,23], polystyrene (PS) [24,25], polypropylene (PP), low-density polyethylene (LDPE), poly(methyl methacrylate) (PMMA), and poly(vinylidene fluoride) (PVDF) [26]. Absorption of up to 21 wt% CO_2 has been reported for high molecular weight PDMS [23]. However, most thermoplastics (e.g. PS and PMMA) have only been reported to show absorption levels up to about 6 wt% [25].

Several techniques have been developed to measure the subsequent viscosity reductions associated with polymer/CO_2 solutions, covering all levels of CO_2 absorption [22–25,27,28]. Falling ball viscometers have been used primarily to measure polymer solutions containing low polymer concentrations (less than 5 wt%) in high levels of absorbed CO_2 (and other supercritical fluids), but are generally limited to low viscosity and low molecular weight solutions [22,29]. High-pressure couette and parallel plate devices, in which a couette or parallel plate geometry was kept in a sealed, high-pressure environment, have been used to measure more viscous melts [30]. Inherent problems with

transferring torque measurements under pressure, primarily because of the use of a dynamic seal that reduces instrument sensitivity, has significantly limited the usefulness of these rheometer designs [28]. Back pressure regulated capillary rheometers and extrusion slit dies, with which a hydrostatic pressure was applied at the capillary or slit exit to maintain a single phase thermoplastic/CO_2 melt, have been utilized to measure viscosities of viscous melts containing low concentrations of absorbed CO_2 [23,25]. An extrusion slit die, with an applied hydrostatic pressure at the die exit, has been used to measure viscosity reductions of polystyrene/nanoclay melts containing absorbed CO_2 [31]. Viscosity reductions for high molecular weight PDMS, PMMA, PVDF, isotactic PP, LDPE and PS melts have been measured using a back pressure regulated capillary rheometer [23,25,26], with up to 80% viscosity reductions reported for polystyrene containing 5 wt% absorbed CO_2 [24].

Despite the existing efforts to absorb CO_2 into thermoplastics and measure the viscosity reduction, none have documented the use of CO_2 to aid in melt processing acrylic copolymers or any other thermally unstable system. More specifically, none of the existing efforts have looked at the equivalent reduction in processing temperature produced by plasticization of acrylic copolymers (or any other thermally unstable polymers) with CO_2. AN copolymers need to be melt processed below temperatures at which the kinetics of the crosslinking reaction become significant, which could be facilitated by the viscosity reduction resulting from CO_2 absorption and plasticization.

The goal of this paper is to establish a framework for the ability of CO_2 to plasticize AN copolymers and facilitate reductions in viscosity and processing temperature. A relatively thermally stable AN copolymer (65 mol% AN) was used as a model system to facilitate absorption and viscosity measurements without significant degradation (crosslinking). The data obtained from this model AN system can then be extended to determine the ability for CO_2 to reduce viscosities and processing temperatures in higher AN content (85 mol% and greater) copolymers where the kinetics of crosslinking become a problem. The ability of this relatively low AN content (65 mol%) acrylic copolymer to absorb CO_2 was determined from differential scanning calorimetry (DSC) and thermogravimetric analyses (TGA). Viscosity effects generated by means of CO_2 absorption were measured using a capillary rheometer modified to allow the application of static pressures at the capillary exit. Equivalent processing temperature differences between the plasticized and pure copolymer were measured. The viscosity data were analyzed using a Williams–Landel–Ferry (WLF) analysis [32], and the absorbance levels were compared to values calculated from Van Krevelen's solubility relationships. An experimentally determined framework was established to estimate the required CO_2 absorption level necessary for a specified reduction in processing temperature (and corresponding viscosity reduction).

2. Experimental

2.1. Materials

An extrudable grade AN/MA copolymer made by BP/Amoco, Barex, was used for this study. Barex is a copolymer containing 65 mol% acrylonitrile (AN), 25 mol% methyl acrylate (MA) and 10 mol% elastomer and is designed to be processed in the temperature range of 180–200 °C. Barex is available in a 4.8 mm long cylindrical pellet of approximately 3.2 mm diameter. Air products medium grade (99.8% pure) carbon dioxide was used for absorption into the Barex copolymer. Air Products 99.998% pure (excluding Argon) nitrogen (N_2) was used to pressurize the exit of the capillary rheometer during viscosity measurements to maintain a single phase melt and prevent the absorbed CO_2 in the polymer melt from flashing off during viscosity measurements. Nitrogen has been shown to be one of the least soluble gases in AN polymers, which possess extremely low gas solubility and diffusivity and were not expected to absorb N_2 [33]. These expectations were confirmed experimentally [34].

2.2. Sample preparation

Barex pellets were saturated with CO_2 in a sealed, constant volume, pressurized bomb for various amounts of time. A Parr instruments model 4760 pressure vessel was used to saturate the Barex samples. Approximately 20 g of polymer were saturated at a time to have sufficient sample for viscosity measurements and thermal analysis. The pressure vessel was initially charged with CO_2 at room temperature in the form of a high pressure gas at 5.86 MPa, and then heated to 120 °C, which increased the pressure to 10.3 MPa. It was necessary to use a saturation temperature above the T_g of the copolymer to increase free volume and ensure dispersion of the CO_2 into the polymer. 120 °C was chosen as the soak temperature because it was well above the T_g of Barex (85 °C) but well below the temperature at which cyclization and crosslinking (thermal degradation) began to occur. Higher temperatures resulted in slight thermal degradation for the longest soak times, and lower temperatures required longer soak times to achieve comparable results. The sample was then held at 120 °C for various amounts of time, corresponding to the 'soak time' for the CO_2 absorption. Following the soak time, the pressurized bomb was cooled back down to room temperature via forced convection. Once cooled to room temperature, the pressure vessel was decompressed over the course of 12 min, corresponding to a decompression rate of 8.27×10^3 Pa/s. The entire heating and cooling process will later be referred to as the 'cycle time' of saturation, which does not include the soak time at 120 °C.

Further high pressure saturations were performed in a similar manner. Following the batch pressurization and heating to 120 °C (corresponding to 10.3 MPa), a Trexel

TR-1-5000L high pressure CO_2 pump was used to directly inject liquid CO_2 into the heated pressure vessel and raise the pressure to 17.2 MPa. This pressure was chosen as the upper limit in this study so that reasonable pressures could be maintained in future extrusion studies.

Following saturation of the Barex copolymer with CO_2, the thermal analyses and rheometry were immediately performed to ensure that no CO_2 was lost from the sample. Samples were prepared and tested as quickly as possible following depressurization and removal from the pressure vessel. The maximum time between depressurization and thermal testing was 15 min, which we found did not result in any significant loss of CO_2 due to diffusion [34]. The polymer pellets were transferred to the rheometer and placed in a pressurized environment within 5 min, again avoiding any significant loss of CO_2 due to diffusion.

2.3. Differential scanning calorimetry

A Seiko model 220 DSC and a TA Instruments model 2920 modulated DSC were used to make the DSC measurements. Heating and cooling rates of 10 °C/min were used. A nitrogen purge was used during measurements in both DSC units. Aluminum pans with pierced lids were used to hold the 5–10 mg samples. The use of pierced lids facilitated the escape of the absorbed CO_2. Glass transition temperatures were calculated using Universal analysis software via the midpoint method.

Two heats were performed on each sample. The first heat allowed direct visualization of the T_g reduction resulting from absorbed CO_2. The second heat verified that no residual CO_2 was present, which was confirmed if the T_g of the pure material was obtained. Samples containing absorbed CO_2 were cooled to −20 °C to further prevent any degassing prior to running the thermal scan, as well as to establish a baseline for easy visualization of the T_g of the plasticized Barex. The test comprised heating from −20 to 180 °C to ensure that all CO_2 had flashed out of the system, cooling back to −20 °C, and then performing the second heat.

In order to ensure that significant CO_2 was not lost between sample decompression and thermal analysis, a calculation was performed to determine the amount of time required to desorb a significant quantity of the absorbed gas (5%), which was found to be several hours due to the extremely low diffusivity of acrylonitrile at room temperature. DSC analysis was used to verify the calculation, which confirmed minimal gas loss within the first 2 h following decompression [34].

2.4. Thermogravimetric analysis

A TA Instruments Hi Res TGA 2950 TGA was used to measure the weight percent of CO_2 that was absorbed into the AN copolymer. A nitrogen purge of 24 ml/min was used. Platinum pans were used to hold 5–10 mg Barex samples containing absorbed CO_2. Measurements were started at room temperature (25 °C) and ramped to 250 °C at a heating rate of 10 °C per minute. Evolution of CO_2 was easily visualized by the weight fraction of the polymer/CO_2 mixture lost following heating through the T_g of the copolymer.

2.5. Pressurized capillary rheometer

An Instron model 3211 capillary rheometer was used to obtain the viscosity of the pure Barex in the temperature range of 180–210 °C and of the plasticized Barex at 180 °C. The rheometer was modified with the addition of a sealed chamber at the capillary exit for the purpose of creating a static pressure to prevent flashing off of the CO_2 from the copolymer, maintaining a single phase melt. The approach of Luxenburg and co-workers [35], used to measure the viscosity of water plasticized soy protein, was extended for this study. A schematic of the experimental apparatus is shown in Fig. 1. A specially constructed pressure assembly was used to apply a constant static pressure to the capillary exit and collect the extrudate during the viscosity measurements. The use of an adjustable pressure relief valve ensured that the applied static pressure remained constant. This was visually verified with a pressure gauge fitted to the pressurized assembly. Nitrogen was used in the range of 3.4–13.8 MPa to apply a static pressure to the capillary exit. The rheometer piston was sealed using Teflon O-rings, and the pressure chamber assembly was sealed to the capillary

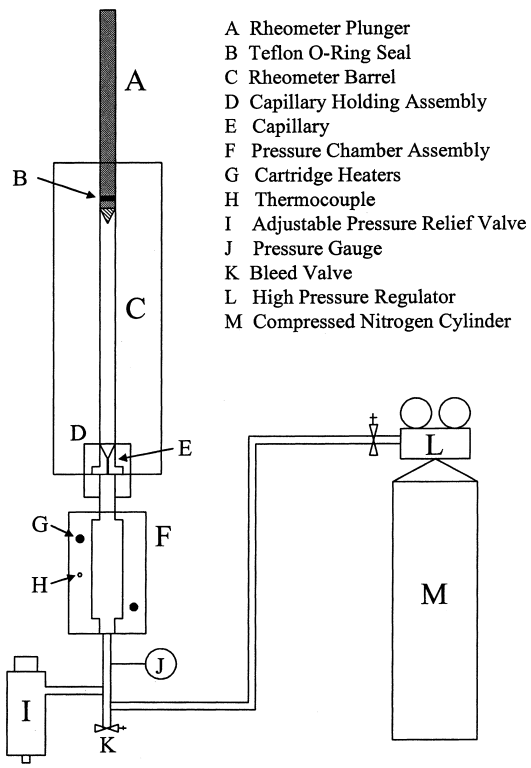

Fig. 1. Schematic of the pressurized capillary rheometer for viscosity measurement of polymers containing absorbed CO_2.

using Teflon spacers. An Omega CN9000 temperature controller was used to control the temperature of the pressurized chamber. Two 150–W Fire Rod cartridge heaters were used to heat and maintain the chamber temperature.

In order to minimize the loss of CO_2 on loading the barrel of the capillary rheometer with pellets containing absorbed CO_2, the following procedure was utilized. The saturated polymer pellets were transferred from the pressure vessel into the cold rheometer and then sealed from the top with the piston. Static pressure was then applied to the capillary exit with the pressure chamber. With the system pressurized, the polymer could be heated to test temperatures without losing the absorbed CO_2 to the atmosphere, and the effects of plasticization on viscosity could be measured.

2.6. Viscosity measurements

Viscosity measurements were performed on Barex-CO_2 materials containing between 2.7 and 6.7 wt% absorbed CO_2. For each Barex-CO_2 sample, measurements were conducted at 180 °C and compared to the pure copolymer viscosity measured at 180 °C. Pure copolymer viscosities were also measured at 190, 200, and 210 °C to provide a set of reference viscosity curves for comparison to the Barex-CO_2 viscosity curves. Measurements at each CO_2 absorption level were conducted with capillaries of 1.0 mm diameter and *L/D* values of 10, 20, and 30, all having a 90° entry angle. Plunger speeds corresponding to shear rates in the range of 5–4000 s^{-1} were used for the measurements.

Viscosity values were obtained by well-known methods from plunger speed and force measurements [36]. In particular, the force required to displace the polymer through the capillary at a constant plunger speed was measured. The actual pressure drop across the capillary (ΔP) was measured as the difference between the upstream force measured by the Instron load cell to push the polymer through the capillary (ΔP_{total}) and the applied static pressure (ΔP_{static}). A correction for the effect of the viscoelastic entry pressure (ΔP_{entry}) was accounted for and determined by the construction of Bagley plots, in which the pressure ($P = \Delta P_{total} - \Delta P_{static} - \Delta P_{friction}$) vs. *L/D* measurements at each shear rate were extrapolated to $P = 0$ and the intercepts were used to determine a set of corrections [36]. The entry pressures determined from the Bagley plots were subtracted from ΔP_{total} to determine the actual pressure drop (ΔP) across the capillary, facilitating determination of a true wall shear stress. The pressure drop correction used to calculate ΔP is defined in Eq. (1):

$$\Delta P = \Delta P_{total} - \Delta P_{static} - \Delta P_{entry} - \Delta P_{friction} \quad (1)$$

where $\Delta P_{friction}$ is the correction to account for the friction imposed by the plunger seal, and was directly measured using an empty sample reservoir at the various plunger speeds and corrected for accordingly at each pressure drop measurement (plunger speed). The wall shear stress, τ, was then calculated using Eq. (2):

$$\tau = \frac{\Delta P}{L}\frac{D}{4} \quad (2)$$

where L and D are the length and diameter of the capillary, respectively. The apparent shear rate, $\dot{\gamma}_a$, was calculated based on the volumetric flow rate of the polymer through the capillary, Q, and the radius of the capillary, R, as defined in Eq. (3):

$$|\dot{\gamma}_a| = \frac{4Q}{\pi R^3} \quad (3)$$

A correction to account for the non-Newtonian nature of the velocity profile in the polymer melt was performed using the classical Rabinowitsch correction to convert from apparent to true shear rate and is shown in Eq. (4) [37]:

$$\dot{\gamma} = \frac{\dot{\gamma}_a}{4}\left(3 + \frac{d\ln\dot{\gamma}_a}{d\ln\tau}\right) \quad (4)$$

The viscosity was then calculated using Eq. (5):

$$\eta = \frac{\tau}{\dot{\gamma}} \quad (5)$$

Effects of the applied static pressure on the viscosity were also considered. To ensure that the applied static pressure did not have an effect on viscosity, the pure copolymer viscosity was measured at 180 °C over the aforementioned shear rate range using applied static pressures of up to 13.8 MPa. These measurements were compared to pure copolymer viscosities measured without applied static pressure to ensure that there were no pressure effects on viscosity.

3. Results and discussion

In the following section, the effects of the amount of absorbed CO_2 on the thermal properties and levels of viscosity reduction of Barex are discussed. Calculated viscosity reductions are then compared to the experimentally measured levels of viscosity reduction (as a function of reduction of T_g) to determine the ability to predict the amount of absorbed CO_2 required for a specified processing temperature reduction. The ability to predict the amount of CO_2 absorption for our saturation conditions is also discussed to determine whether the level of CO_2 absorption can be determined for any given set of saturation conditions.

3.1. Thermal analysis

DSC and TGA thermal analyses were used to establish a relationship between the reduction of T_g and the amount of absorbed CO_2 for a given soak time and pressure. Figs. 2 and 3 show the DSC and TGA scans of Barex following CO_2 absorption at 120 °C and both saturation pressures, 10.3 and 17.2 MPa. The data collected for both heats are

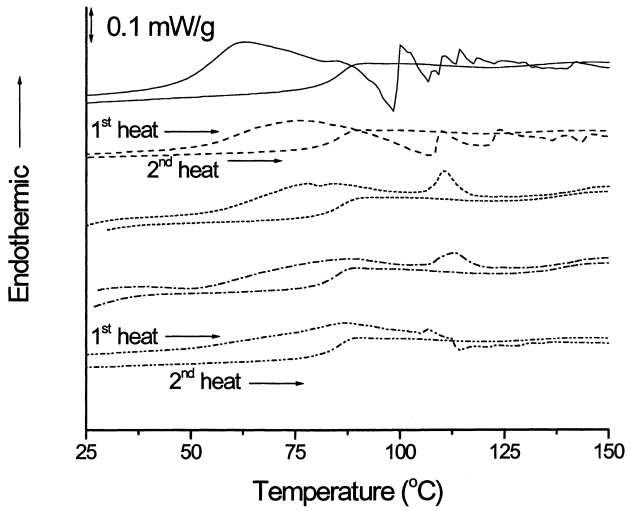

Fig. 2. DSC scans of Barex saturated at 120 °C for various times at 10.3 and 17.2 MPa CO_2. From top to bottom: (—) 6 h, 17.2 MPa; (– –) 6 h, 10.3 MPa; (- - -) 4 h, 10.3 MPa; (– - –) 2 h, 10.3 MPa; (– - - –) 0 h, 10.3 MPa.

depicted in the figures for easy visualization of the T_g difference between plasticized and pure Barex (meaning pure in the sense that no residual CO_2 remains). The first heat of the polymer containing CO_2 is represented by the upper curve for each sample, and the second heat (following cool down) is represented by the lower curve. Using only the aforementioned cycle time, a T_g reduction of 15 °C was obtained, corresponding to a 2.7 wt% uptake of CO_2. These results are indicated by the 0 h soak time in the DSC and TGA scans shown in Figs. 2 and 3. Longer soak times at 10.3 MPa (120 °C) resulted in greater reductions of T_g. A 6 h soak resulted in a reduction of T_g of 21 °C, corresponding to a 4.7 wt% uptake in CO_2. Beyond the 6 h soak, no additional uptake of CO_2 was observed. The TGA results

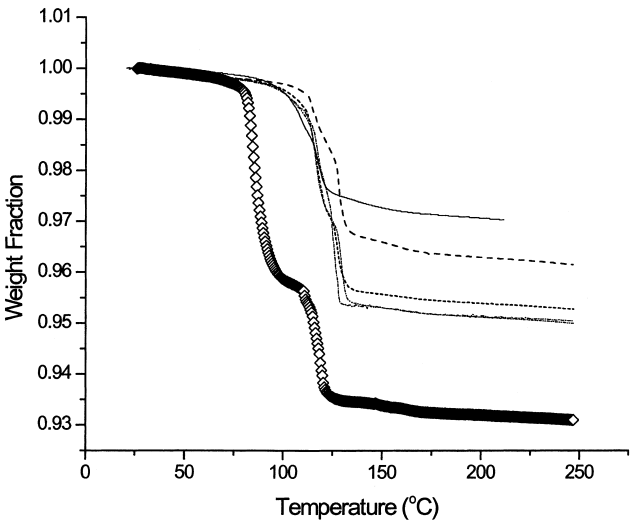

Fig. 3. TGA of Barex comparing 10.3 and 17.2 MPa CO_2 soak pressures. Soak temperature was 120 °C. 10.3 MPa soak times (from top to bottom): (—) 0, (– –) 2, (- - -) 4, (– - –) 6, and (– - - –) 12 h. 6 and 12 h soak times overlap. (◇) 6 h, 17.2 MPa soak.

shown for the 12 h soak in Fig. 3 clearly indicate that no additional CO_2 was absorbed over the 6 h saturation. Saturation times in excess of 12 h caused the polymer to degrade to a very slight extent, indicated by a slight change in the polymer color.

Thermal analysis of the sample saturated at 17.2 MPa was only performed using the 6 h soak time at 120 °C because no significant absorption was observed using longer soak times in the 10.3 MPa saturation experiments. As seen from the DSC results in Fig. 2, the glass transition temperature was reduced by 31 °C (to 54 °C), corresponding to a 6.7 wt% CO_2 uptake, as indicated by the TGA scans in Fig. 3.

Combining the thermal analysis data from the DSC and TGA results in Figs. 2 and 3 facilitated an estimate of the amount of CO_2 required to achieve a desired T_g reduction, which is shown in Fig. 4. The dashed line is an exponential fit of the compiled data, and quite accurately represents the measured range of CO_2 absorption and corresponding T_g reduction levels. The exponential fit of the data is represented in Eq. (6):

$$T = 9.1\exp[0.2W] \tag{6}$$

where T is the reduction in glass transition temperature (°C) resulting from CO_2 absorption and W is the weight percent uptake of CO_2. The fit of the data permits a determination of the amount of CO_2 required to obtain a reduction of T_g within the range of measured data, which will be necessary once a required viscosity reduction is known.

3.2. Viscosity reduction

The ability of CO_2 to reduce the viscosity of Barex was determined by measuring the viscosity vs. shear rate for Barex containing absorbed CO_2. Viscosity values were obtained at 180 °C for both the pure and plasticized Barex and were compared to determine the magnitude of the viscosity reduction (at 180 °C) obtained from CO_2 absorption at each absorption level. The viscosity values of the lowest and highest absorption percentages from the 10.3 MPa saturations (2.7 and 4.7 wt% CO_2, corresponding to a 15 and 21 °C T_g reduction, respectively) and the viscosity values for the highest absorption level at the 17.2 MPa saturation pressure (corresponding to a 6.7 wt% absorption and 31 °C T_g reduction) were measured.

Bagley plots were constructed for both the pure and plasticized (containing 6.7 wt% CO_2) Barex samples for the highest, lowest, and an intermediate measured shear rate, as shown in Fig. 5. The Bagley plots clearly indicate linear pressure dependences over the range of shear rates tested for both pure and plasticized Barex, with correlation coefficients greater than 0.99 for the linear fits at each shear rate. These results indicate that viscous heating (which would be indicated by a downward curving slope) was not occurring, and that the viscosity was not pressure dependent (which would be indicated by an upward curving slope).

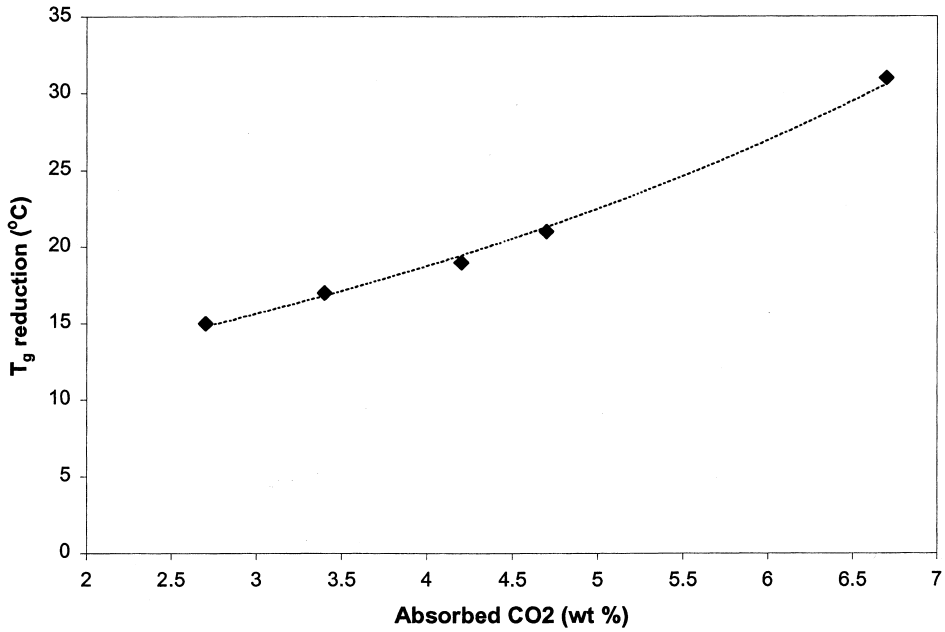

Fig. 4. T_g reduction as a function of level of absorbed CO_2. (◆) DSC/TGA data. (- -) exponential fit.

Differences in the slopes and intercepts of the Bagley plots between pure and plasticized Barex were analyzed. The slope of each linear fit in the Bagley plots, which is directly proportional to the shear stress at each shear rate, was expected to decrease for plasticized Barex, assuming the viscosity decreased upon absorption of CO_2. As expected, the slope at any given shear rate for plasticized Barex in Fig. 5 is lower than that for pure Barex, indicating a lower shear stress and, therefore, a lower viscosity. Entry pressures were obtained from the intercepts (at $L/D = 0$) of the Bagley plots, and the viscosity data for both pure and plasticized Barex at 180 °C were corrected for entry pressure at each shear rate accordingly (as described in Eq. (1)). It is interesting that the entry pressures for the plasticized Barex were higher than those determined for pure Barex, because we expected that as the viscosity levels were decreased, the entry pressures would decrease in a similar manner. To check for consistency between the linear fit of the pressure drop vs. L/D data and the calculated pressure drops (from Eq. (1)), the wall shear stresses were

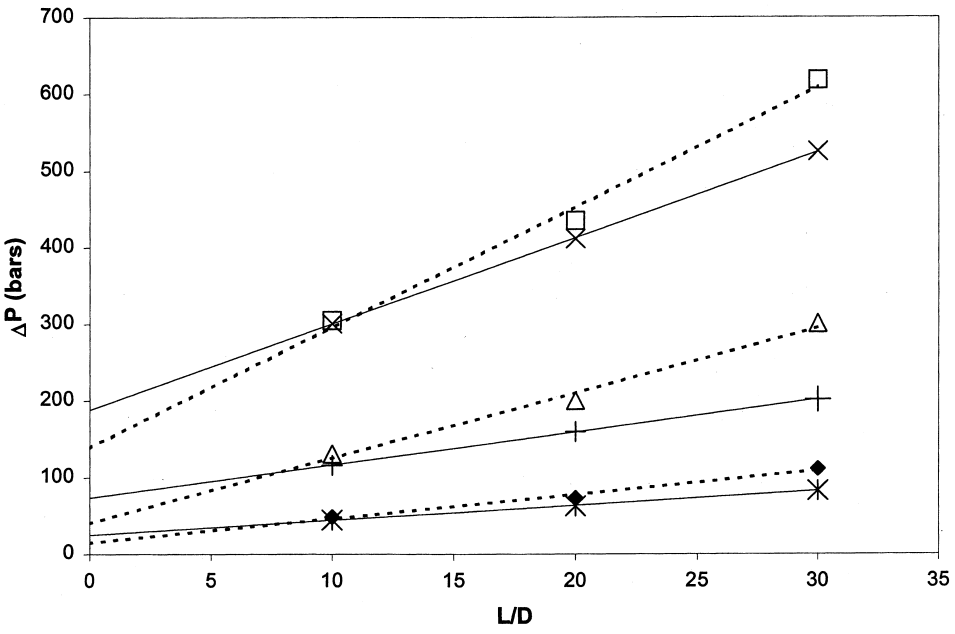

Fig. 5. Bagley plots for pure and plasticized (containing 6.7 wt% CO_2) Barex at 180 °C and L/D values of 10, 20, and 30. Capillary diameter 1.0 mm. Pure copolymer apparent shear rates: (◆) 7 s^{-1}, (△) 73 s^{-1}, (□) 1210 s^{-1}. Saturated copolymer apparent shear rates: (*) 7 s^{-1}, (+) 73 s^{-1}, (×) 1210 s^{-1}. Dashed lines represent linear fits of the data for pure Barex at the above shear rates. Solid lines are linear fits of the plasticized Barex data.

calculated at each shear rate using the slope of the Bagley plots (τ = slope/4). The data are plotted in Fig. 6, and over the range of measured shear rates, the shear stresses obtained from the slopes of the Bagley plots were found to be within +/− 0.5% of the shear stresses calculated using Eqs. (1) and (2). The origin of the higher entry pressures in Barex containing absorbed CO_2 is unknown, but it is possible that absorbed CO_2 may have an effect on the extensional rheology of Barex, and correspondingly affects the entry pressures in an unexpected manner.

Viscosity reductions at each CO_2 absorption level are indicated by the viscosity vs. shear rate data in Fig. 7, which shows a general trend of greater viscosity reduction for an increase in the amount of adsorbed CO_2. The viscosity vs. shear rate data in Fig. 7 is for a *L/D* of 30, but almost identical results were obtained for the other *L/D* values. An average viscosity reduction of 7% was obtained for the plasticized Barex containing 2.7 wt% absorbed CO_2 over the range of shear rates tested. Increasing the amount of absorbed CO_2 to 4.7 wt% had a significant effect on the viscosity reduction, resulting in an average reduction in viscosity of 32%. Finally, the sample containing 6.7 wt% absorbed CO_2 exhibited a viscosity reduction of about 60%, which is approximately equivalent to a three fold viscosity reduction.

To ensure that the applied static pressure was ample to prevent foaming, the extrudate of the plasticized Barex was examined using a scanning electron microscope (SEM). As seen in Fig. 8, the extrudate showed signs of bubble nucleation, but there was no indication of significant bubble growth. This suggests that the applied static pressure was sufficient to prevent foaming and loss of the CO_2 from the plasticized melt in the rheometer barrel, ensuring a relatively homogeneous melt. Visual inspection of the extrudate processed at lower applied static pressures revealed a milky, cloudy extrudate, which was not observed in the extrudate used to obtain the cross section shown in Fig. 8.

3.3. Equivalent processing temperature reductions

In order to determine the ability for small amounts of absorbed CO_2 to reduce the processing temperature, the viscosity of Barex containing absorbed CO_2 at 180 °C was compared to the pure copolymer viscosity measured at higher temperatures. For each absorption level, the temperature was found where the pure copolymer viscosity overlapped the plasticized copolymer viscosity measured at 180 °C. The difference between these two temperatures corresponded to a potential equivalent processing temperature difference. Pure copolymer viscosities were measured at temperatures in the range 190–210 °C for comparison to the plasticized copolymer. Although not shown, all pure copolymer viscosity data at the elevated temperatures were obtained at three *L/D* values to obtain a correction for the entry pressure. Bagley plots were constructed for the pure copolymer at the elevated testing temperatures and indicated linear pressure dependences, similar to that observed for the pure copolymer at 180 °C in Fig. 5.

Equivalent processing temperature reductions were determined for the three CO_2 absorption levels studied. The resulting overall viscosity reduction for the 2.7 wt% CO_2 uptake was relatively small. Consequently, the temperature difference in viscosity was only a few degrees, and it was difficult to establish a statistical difference. Viscosity reductions from the 4.7 and 6.7 wt% CO_2

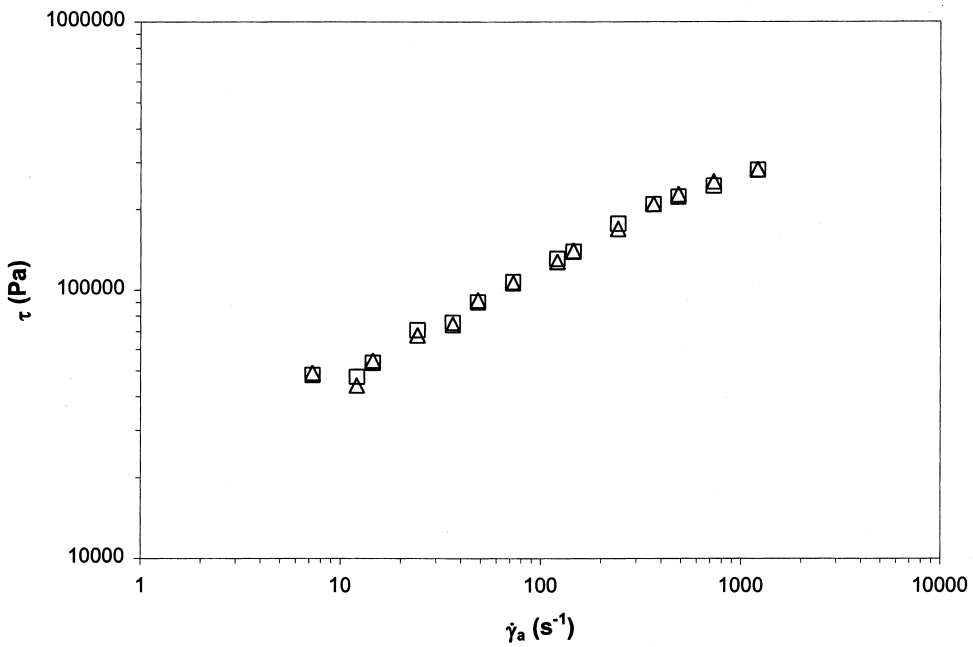

Fig. 6. Shear stress for saturated Barex containing 6.7 wt% CO_2 calculated from: (□) slopes of linear fit in Bagley plots of Fig. 5; (△) Eqs. (1) and (2).

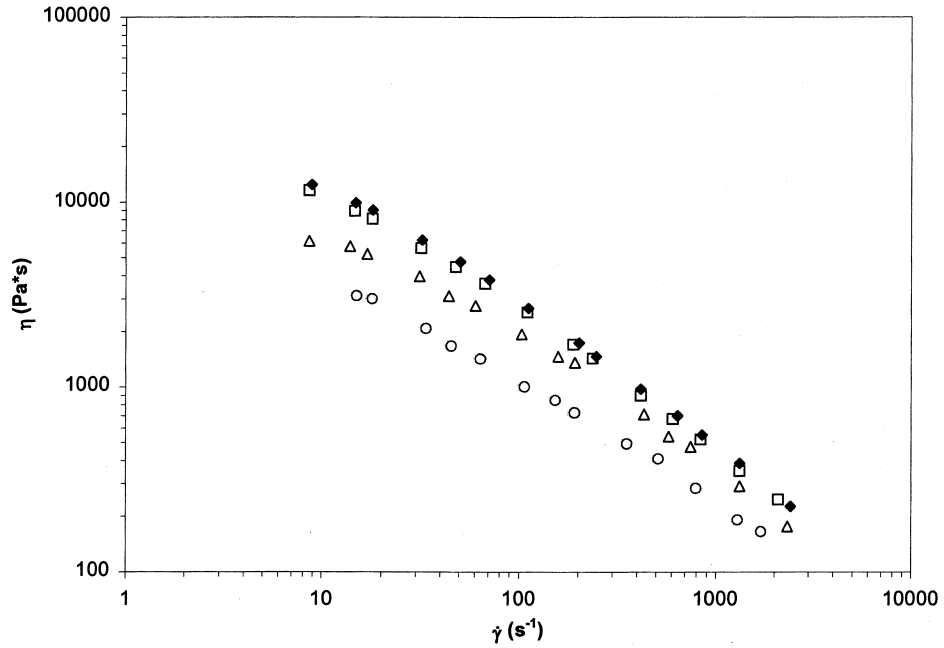

Fig. 7. Viscosity vs. shear rate data of Barex containing (□) 2.7, (△) 4.7, and (○) 6.7 wt% CO_2. (◆) pure Barex. $L/D = 30$, 1.0 mm diameter. $T = 180$ °C.

absorptions were much more significant. The viscosity vs. shear rate behavior of the pure copolymer at 180 and 190 °C is compared to the plasticized polymer containing 4.7 wt% CO_2 at 180 °C in Fig. 9. Viscosity levels of Barex containing 4.7 wt% absorbed CO_2 at 180 °C overlap the viscosity obtained for the pure copolymer at 190 °C, which correlates to an equivalent 10 °C difference in processing temperature between the pure and plasticized copolymer. Only the data collected for the *L/D* of 20 is shown in Fig. 9 to facilitate clear visualization of the viscosity overlap, but similar results were obtained for all three tested *L/D* values. The viscosity levels of the pure copolymer at 180 and 210 °C are compared to that of the saturated copolymer containing 6.7 wt% CO_2 at 180 °C in Fig. 10. The saturated copolymer viscosity levels at 180 °C overlap the viscosity vs. shear rate data of the pure copolymer at 210 °C, suggesting an equivalent 30 °C difference in processing temperature between the pure and plasticized copolymer. The amount of absorbed CO_2 is only increased by approximately 40% over the 4.7 wt% absorption, yet the viscosity reduction is doubled and the equivalent difference in processing temperature is tripled. These trends suggest that the relationship between CO_2 absorption level (T_g reduction) and viscosity reduction is nonlinear.

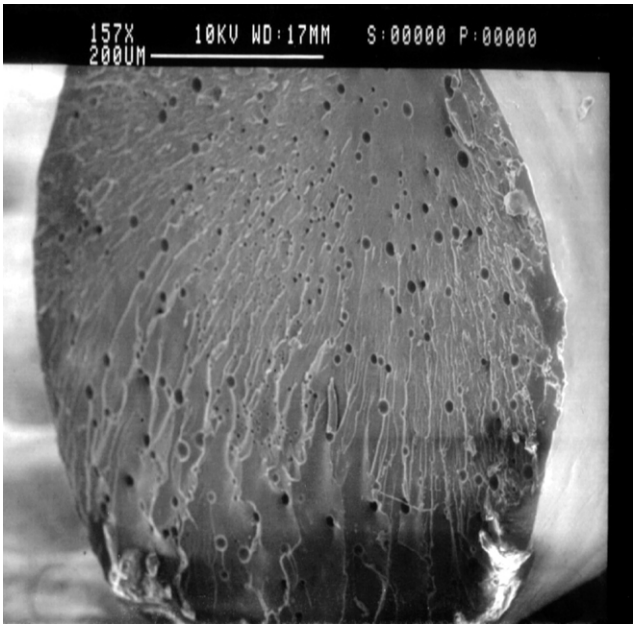

Fig. 8. SEM of Barex containing 4.7 wt% absorbed CO_2 extruded into the pressurized chamber at 180 °C. Extrudate is approximately 500 μm in diameter.

3.4. WLF analysis

To obtain a specified reduction in processing temperature, a reduction of T_g is necessary to sufficiently reduce the viscosity. We evaluated the ability of the WLF equation to predict viscosity reductions based on the measured reductions of T_g for Barex. If the values were in agreement with the measured viscosity reductions, then the WLF analysis could be similarly utilized to predict a required reduction of T_g (based on a specified viscosity reduction or required processing temperature reduction). The WLF equation, which relates the viscosity at a temperature T, η_T, to the viscosity at T_g, η_{T_g}, is shown in Eq. (7) [32].

$$\log \frac{\eta_T}{\eta_{T_g}} = \frac{C_1(T - T_g)}{C_2 + (T - T_g)} \tag{7}$$

Writing the WLF equation for the pure and plasticized copolymers and taking the ratio of the two equations

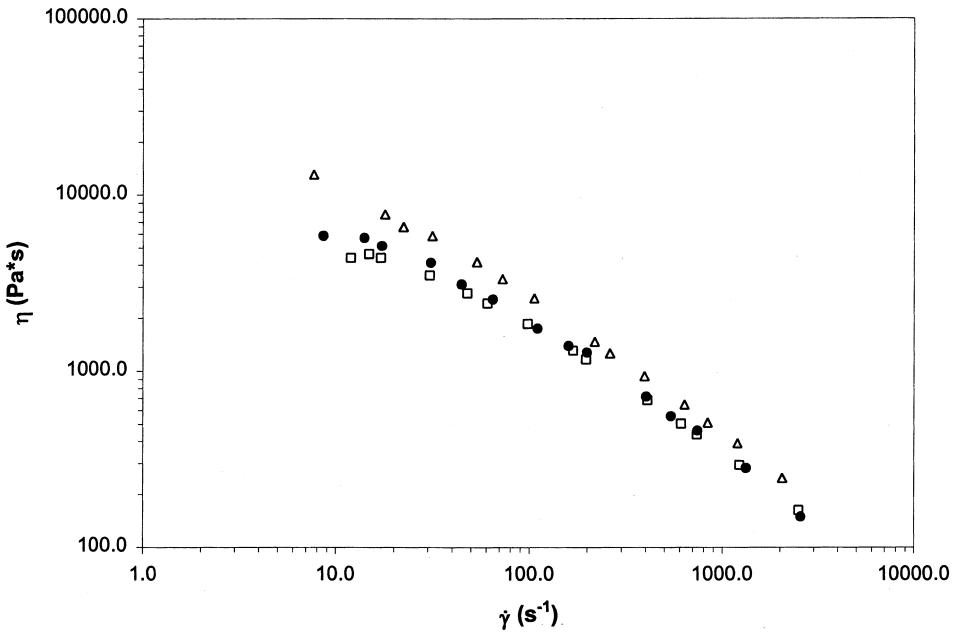

Fig. 9. Comparison of viscosity of Barex containing 4.7 wt% CO_2 at 180 °C (●) to that of pure Barex at 190 °C (□). (△) pure Barex viscosity at 180 °C. $L/D = 20$. 1.0 mm capillary diameter.

resulted in a single equation that relates the glass transition temperature of the pure and plasticized copolymers to the viscosity reduction, as shown in Eq. (8):

$$\frac{\eta(T_1)^{(1)}}{\eta(T_1)^{(2)}} = \frac{10^{\left(\frac{-C_1(T_1-T_g^{(1)})}{(C_2+T_1-T_g^{(1)})}\right)}}{10^{\left(\frac{-C_1(T_1-T_g^{(2)})}{C_2+T_1-T_g^{(2)}}\right)}} \tag{8}$$

where $\eta(T_1)^{(1)}$ and $\eta(T_1)^{(2)}$ are the viscosities of the pure and plasticized copolymer, respectively, at a given test temperature T_1, and $T_g^{(1)}$ and $T_g^{(2)}$ are the glass transition temperatures of the pure and plasticized copolymers, respectively, obtained from DSC measurements. Eq. (8) was used with the universal constants $C_1 = 17.44$ and $C_2 = 51.6$ °K to estimate a viscosity reduction based on the DSC measured T_g values for plasticized Barex (from Fig. 2) and pure Barex ($T_g = 85$ °C). As seen in Fig. 11, the predicted viscosity reduction from Eq. (8) has a nonlinear relationship

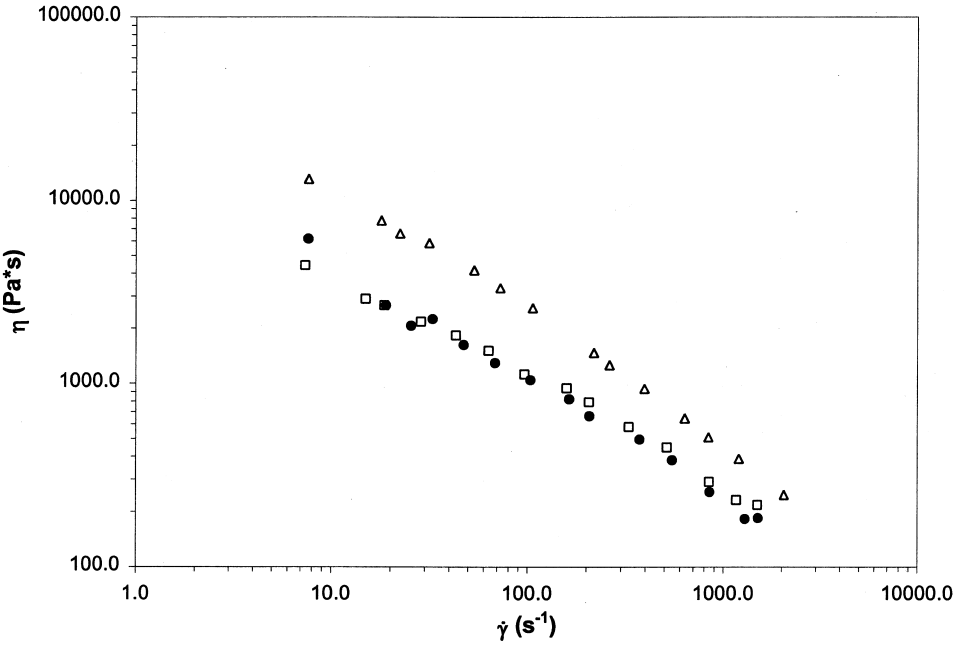

Fig. 10. Comparison of viscosity of Barex containing 6.7 wt% CO_2 at 180 °C (●) to that of Barex at 210 °C (□). (△) pure Barex viscosity at 180 °C. $L/D = 20$. 1.0 mm capillary diameter.

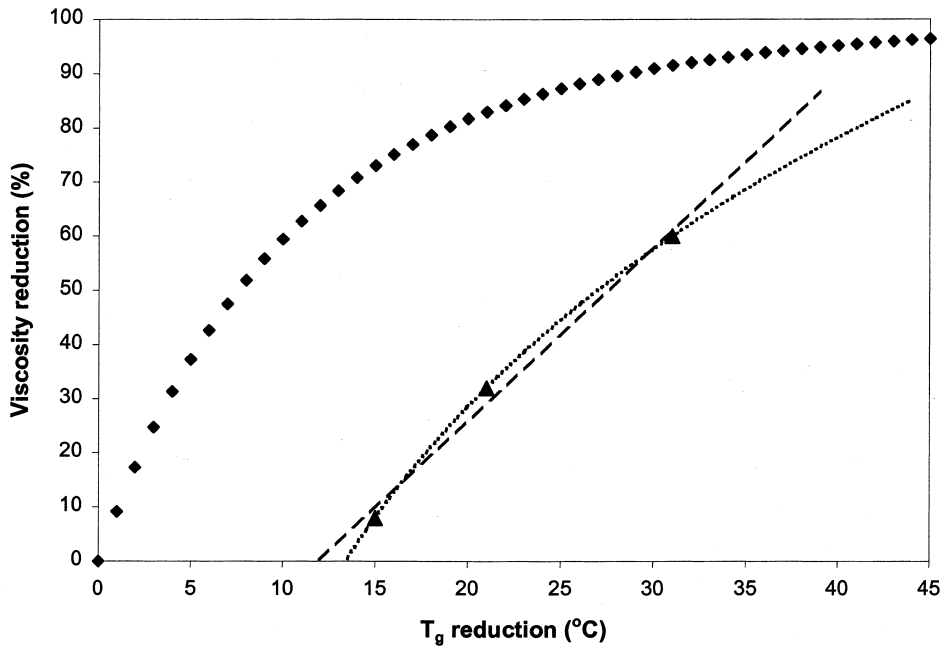

Fig. 11. Viscosity reduction for plasticized Barex T_g reduction: (◆) calculated values using Eq. (8) and universal constants; (▲) measured values; (– –) linear fit of experimental data, (- - -) logarithmic fit of experimental data.

to the reduction in T_g. Linear and logarithmic fits of the measured data in Fig. 11 resulted in correlation coefficients of 0.99 and 1.0, respectively, suggesting a nonlinear logarithmic relationship between the experimentally measured viscosity reduction and the reduction of T_g. However, the values of the measured viscosity reduction are lower than the predicted values for a given reduction of T_g.

Two possible sources of error, namely pressure effects on viscosity and the assumption of universal constants, were addressed to explain the discrepancy between the measured and calculated viscosity reductions. To ensure that pressure effects on viscosity were not creating a discrepancy, the pure copolymer viscosity was measured with applied static pressures (at the capillary exit) of 6.9 and 13.8 MPa. The reason for concern was that polymers such as polystyrene have been shown to have a viscosity that is pressure sensitive, which leads to a discrepancy between the measured and predicted viscosity reductions [24]. As seen from the data in Fig. 12, the copolymer viscosity was unaffected by the application of static pressure at the capillary exit. These results suggest that the applied static pressure had no significant effect on the measured pressure drops and did not contribute any significant source of error over the range of pressures used. As a result, we concluded that the primary source of error between the WLF analysis and the experimentally measured values was attributable to the use of universal constants for C_1 and C_2 in Eq. (8).

Another possible contribution to the error was the temperature range utilized with the WLF analysis. The useful range of the WLF analysis is $T_g + 100\,^{\circ}C$ [32]. Viscosity measurements were obtained at temperatures of up to $T_g + 126\,^{\circ}C$. Hence, the analysis may have been used just outside the range of the WLF equation, which may have also contributed to the discrepancy between calculated and measured viscosity reductions.

The WLF analysis was not able to accurately predict the viscosity reduction based on the measured viscosity values and glass transition temperatures for pure and plasticized Barex, and as a result cannot be used with the universal constants to accurately predict a reduction of T_g for a specified viscosity reduction. We believe that determining a reference temperature, T_o, for use in place of T_g in the WLF analysis, would facilitate a relationship between reductions of T_g to viscosity reductions. T_o would be obtained by a best fit of the experimental viscosity data to a master curve, using the constants $C_1 = 8.86$ and $C_2 = 101.6\,^{\circ}K$ in Eq. (8) [37]. This analysis still requires experimental data, and only facilitates prediction of intermediate values of reductions of T_g as a function of viscosity reduction over the measured range of data.

3.5. Absorption predictions

We next examined the ability to predict the saturation conditions necessary to obtain a specific amount of absorbed CO_2 in Barex. If the saturation conditions required to absorb a specific amount of CO_2 in Barex can be predicted, then the resulting reduction of T_g, viscosity reduction, and ultimately reduction in processing temperature can be determined based only on the temperature and pressure of saturation (assuming that the WLF analysis can be made to work). We calculated the solubility of CO_2 in Barex to determine a relative volume fraction of plasticizer (or diluent) per volume of solution, which was converted to weight percent

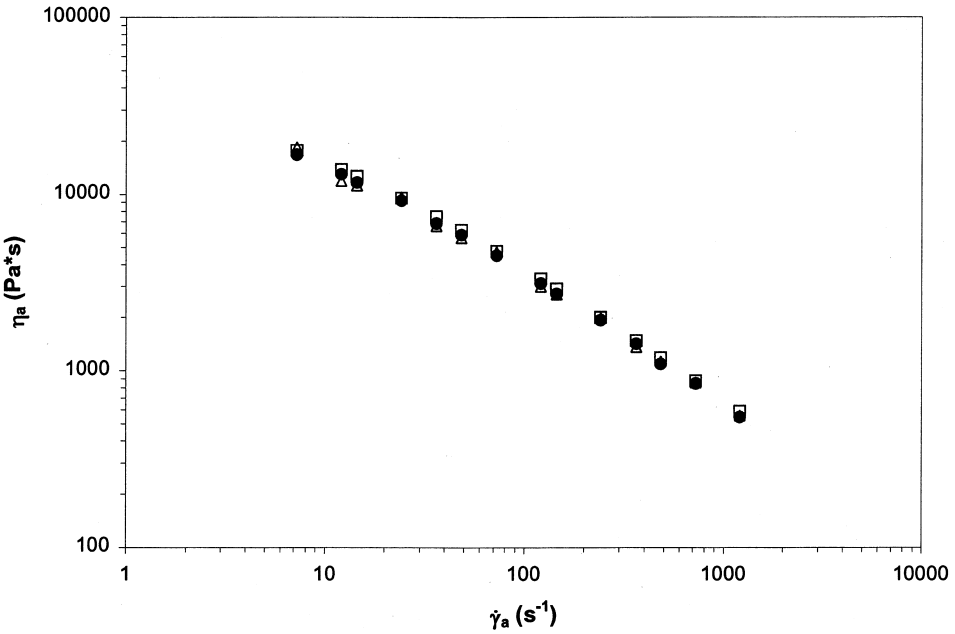

Fig. 12. Apparent viscosity of pure AN copolymer at 180 °C. (△) 13.8 MPa applied static pressure; (●) 6.9 MPa applied static pressure; (□) no applied static pressure.

by the use of an equation of state. These solubility calculations were performed to determine whether the measured amount of absorbed CO_2 agreed with the predicted absorption levels. If the values were in agreement, then we expect that absorption levels for other saturation temperatures and pressures could be predicted. We used Van Krevelen's empirical relationships to determine the solubility of CO_2 in Barex [38]. Van Krevelen determined empirical relationships for solubility of gases in both glassy amorphous polymers and polymers in the rubbery state [38]. Each set of relationships was evaluated to predict solubility for our polymer/CO_2 system, and the volume of absorbed CO_2 per volume of solution was accordingly calculated. The Sanchez–Lacombe equation of state, which is known to accurately predict the physical properties of near critical and supercritical gases, was then used to calculate the density of the CO_2 at the saturation conditions, facilitating conversion of the calculated volume fraction of absorbed gas into a weight percent [39].

As a first approximation, the amount of absorbed CO_2 can be related to the absorption pressure and polymer solubility by the relationship in Eq. (9):

$$\frac{V_A}{V_P} = SP \tag{9}$$

where V_A is the volume of CO_2 dissolved into Barex per unit volume of solution, V_P is the volume of Barex per unit volume of solution, P is the pressure of saturation, and S is the solubility of Barex, which can be estimated with an Arrhenius type expression as follows in Eq. (10) [40]:

$$S = S_0 \exp\left(\frac{-\Delta H_S}{RT}\right) \tag{10}$$

where ΔH_S is the molar heat of sorption in J/mol, and S_o is a pre-exponential factor in cm^3/cm^3 Pa. The molar heat of sorption and pre-exponential terms are not readily found, but can be estimated by Van Krevelen's relationships to Lennard Jones temperature (ε/k) of the gas [38]. For elastomers and polymers in the rubbery state, Van Krevelen determined the empirical relationships shown in Eqs. (11) and (12):

$$10^{-3}\frac{\Delta H_S}{R} = 1.0 - 0.010\frac{\varepsilon}{k} \pm 0.5 \tag{11}$$

$$\log S_0 = -5.5 - 0.005\frac{\varepsilon}{k} \pm 0.8 \tag{12}$$

For CO_2, the Lennard Jones temperature is 195.2 K [38]. The mean solubility was calculated to be 3.4E-6 cm^3/cm^3 Pa, which is similar to reported solubilities for other thermoplastics in the rubbery state [41]. For glassy amorphous polymers, Van Krevelen arrived at the empirical relationships in Eqs. (13) and (14):

$$10^{-3}\frac{\Delta H_S}{R} = 0.5 - 0.010\frac{\varepsilon}{k} \pm 1.2 \tag{13}$$

$$\log S_0 = -6.65 - 0.005\frac{\varepsilon}{k} \pm 1.8 \tag{14}$$

which resulted in a mean calculated solubility of 9.5E-7 cm^3/cm^3 Pa. To convert the volume of CO_2 into a weight fraction, the density was required at the saturation temperature and pressure. The Sanchez–Lacombe equation of state (S–L EOS) is well known to accurately represent the physical properties of CO_2 in both near critical and supercritical states [42]. The EOS is based on a statistical mechanics derivation and relates pressure, density, and

temperature as follows in Eq. (15):

$$\frac{P}{T} = -\ln(1-\rho) - \left(1 - \frac{1}{r}\right)\rho - \frac{\rho^2}{T} \quad (15)$$

where P, T, and ρ are reduced pressure, temperature, and density, respectively, with respect to characteristic parameters, and r is the number of lattice sites occupied by a molecule of molecular weight M. The characteristic P, T, and ρ parameters are provided for CO_2 by Garg et al. [19]. Densities of 32.6 and 55.4 kg/m^3 were calculated for CO_2 at 10.3 and 17.2 MPa, respectively, and 120 °C.

By assuming that the volume of polymer is approximately the same as the volume of solution, Eq. (9) was solved for the mass fraction of CO_2. Using Eqs. (11) and (12) for a polymer in the rubbery state, it was estimated that approximately 50 and 74 wt% CO_2 were expected to absorb at 10.3 and 17.2 MPa, respectively, for the 120 °C saturation. Using Eqs. (13) and (14) for a glassy amorphous polymer estimated that approximately 22 and 45 wt% CO_2 would absorb at 10.3 and 17.2 MPa, respectively, for the 120 °C saturation. For comparison, 4.7 and 6.7 wt% CO_2 were experimentally measured for the Barex copolymer. DMTA results indicated that Barex was indeed in the rubbery state during the saturation, and the calculation using mean solubility for a rubbery polymer over predicted the experimentally determined values of absorption [34].

When using the Van Krevelen relationships, the sensitivity of S_o and $\Delta H_S/R$ in Eqs. (11)–(14) must be considered. Recalculating the solubility by using the equations for a polymer in the rubbery state, at the upper limit of the range of statistical error of Eq. (11) and the lower limit of Eq. (12), and again solving for the volume of CO_2, indicated that 4.8 and 12.6 wt% CO_2 were expected to absorb into the polymer at 10.3 and 17.2 MPa, respectively, for the saturation carried out at 120 °C. These values more closely matched the experimentally measured absorption levels and, in fact, the 10.3 MPa saturation was almost exactly predicted. For comparison, recalculating the absorption values at the upper limit of the range of statistical error of Eq. (13) and the lower limit of Eq. (14) (for a glassy amorphous polymer), resulted in expected absorptions of less than 1 wt% for both pressures at 120 °C. These results suggest that the Van Krevelen relationships for a polymer in the rubbery state can be used in conjunction with the Sanchez–Lacombe EOS to accurately predict absorption levels for other saturation conditions with Barex. However, the statistical error in Eqs. (11)–(14) provides a large range of values possible when calculating S_o and $\Delta H_S/R$ for the polymer. As a result, the upper limit of the range of statistical error of Eq. (11) and the lower limit of Eq. (12) must be used when predicting absorption levels for Barex (in the rubbery state).

4. Conclusions

This study has shown that an AN copolymer, Barex, has the ability to absorb CO_2 and exhibit a reduction in its T_g of up to 31 °C. The corresponding amount of absorbed CO_2 was up to 6.7 wt% CO_2 using the 6 h. saturation at 17.2 MPa. The accompanying viscosity reduction was measured to be up to 60% at the highest CO_2 absorption level, corresponding to an equivalent processing temperature reduction of 30 °C. The WLF analysis, when used with universal constants, was not suitable for predicting the reduction of T_g required for a specific viscosity reduction. Within the statistical limits of error, Van Krevelen's solubility relationships for a polymer in the rubbery state can be used to predict the amount of absorbed CO_2 expected for a given set of saturation conditions. The upper limit of the range of statistical error for calculation of $\Delta H_S/R$, and the lower limit for calculating S_o, must be used to accurately predict solubility values for Barex. As a result of the discrepancy in the WLF analysis, we could not theoretically predict the T_g reduction as a function of viscosity reduction. Therefore, experimentally measured T_g and viscosity data are required to determine saturation conditions necessary to obtain a specific processing temperature reduction. Future work will extend to higher AN content copolymers, where the kinetics of crosslinking will become a problem, to determine the dependence of AN content on CO_2 absorption and plasticization.

Acknowledgements

The authors wish to thank the U.S. Environmental Protection Agency (EPA) Science to Achieve Results (STAR), program grant #R-82955501-0, for financial support.

References

[1] Rangarajan P, Yang J, Bhanu V, Godshall D, McGrath J, Wilkes G, Baird D. J Appl Polym Sci 2002;85(1):69–83.
[2] Riggs DM, Shuford RJ, Lewis RW. Handbook of composites. New York: Van Nostrand Reinhold; 1982. Chapter 11.
[3] Bhanu VA, Wiles KB, Rangarajan P, Glass TE, Godshall D, Sankarpandian M, Baird DG, Wilkes GL, Banthia AK, McGrath JE. Abstr Pap Am Chem Soc 2001;U332.
[4] Gupta AK, Paliwal DK, Bajaj P. J Macro Sci-Rev Macro Chem Phys 1991;C31(1):1–89.
[5] Min BG, Son TW, Kim BC, Jo WH. Polym J 1992;24(9):841–8.
[6] Bhanu VA, Rangarajan P, Wiles K, Bortner M, Sankarpandian M, Godshall D, Glass TE, Banthia AK, Yang J, Wilkes G, Baird D, McGrath JE. Polymer 2002;43(18):4841–50.
[7] Rangarajan P, Bhanu VA, Godshall D, Wilkes GL, McGrath JE, Baird DG. Polymer 2002;43(9):2699–709.
[8] Coxe CD. US Patent US 2,585,444; 1952.
[9] Frushour BG. Polym Bull 1982;71–8.
[10] Daumit GP, Ko YS, Slater CR, Venner JG, Young CC. US Patent US 4,921,656; 1990.

[11] Daumit GP, Ko YS, Slater CR, Venner JG, Young CC, Zwick MM. US Patent US 4,981,752; 1991.
[12] Atureliya SK, Bashir Z. Polymer 1993;34(24):5116–22.
[13] Porosoff H. US Patent US 4,163,770; 1979.
[14] DeMaria F, Young CC. US Patent US 4, 303, 607; 1981.
[15] Pfeiffer RE, Peacher SE. US Patent US 4,318,680; 1982.
[16] Grove D, Desai P, Abhiraman AS. Carbon 1988;26(3):403–11.
[17] Cooper A, Howdle S. Mat World 2000;8(5):10–12.
[18] Moore S, Samdani S, Ondrey G, Parkinson G. Chem Engng 1994; 101(3):32–4.
[19] Garg A, Gulari E, Manke CW. Macromolecules 1994;27(20): 5643–53.
[20] Shieh YT, Su JH, Manivannan G, Lee PHC, Sawan SP, Spall WD. J Appl Polym Sci 1996;59(4):707–17.
[21] Shieh YT, Su JH, Manivannan G, Lee PHC, Sawan SP, Spall WD. J Appl Polym Sci 1996;59(4):695–705.
[22] Bae YC, Gulari E. J Appl Polym Sci 1997;63(4):459–66.
[23] Gerhardt LJ, Manke CW, Gulari E. J Polym Sci Part B-Polym Phys 1997;35(3):523–34.
[24] Royer JR, Gay YJ, DeSimone JM, Khan SA. J Polym Sci Part B-Polym Phys 2000;38(23):3168–80.
[25] Kwag C, Manke CW, Gulari E. J Polym Sci Part B-Polym Phys 1999; 37(19):2771–81.
[26] Royer JR, DeSimone JM, Khan SA. J Polym Sci Part B-Polym Phys 2001;39(23):3055–66.
[27] Lee M, Park CB, Tzoganakis C. Polym Engng Sci 1999;39(1): 99–109.
[28] Royer JR, Gay YJ, Adam M, DeSimone JM, Khan SA. Polymer 2002; 43(8):2375–83.
[29] Kiran E, Gokmenoglu Z. J Appl Polym Sci 1995;58(12):2307–24.
[30] Koran F, Dealy JM. J Rheol 1999;43(5):1279–90.
[31] Wingert MJ, Han X, Li H, Zeng C, Lee LJ, Tomasko DL, Koelling KW. Proc Soc Plast Engng ANTEC 2003. pp. 986–990.
[32] Ferry JD. Viscoelastic properties of polymers. New York: Wiley; 1980.
[33] Chiou JS, Paul DR. J Polym Sci Part B-Polym Phys 1987;25(8): 1699–707.
[34] Bortner MJ. PhD Dissertation, Virginia Tech; 2003.
[35] Luxenburg LA, Baird DG, Joseph EG. Biotech Prog 1985;1(1):33–7.
[36] Macosko CW. Rheology: principles, measurements, and applications. New York: VCH; 1994.
[37] Bird RB, Armstrong RC, Hassager O. Dynamics of polymeric liquids v. 1: fluid mechanics, 2nd ed. New York: Wiley; 1977.
[38] van Krevelen DW. Properties of polymers: their correlation with chemical structure, their numerical estimation and prediction from additive group contributions. Elsevier: Amsterdam; 1990.
[39] Sanchez IC, Lacombe RH. Macromolecules 1978;11(6):1145–56.
[40] Baird DG, Collias DI. Polymer processing: principles and design. New York: Wiley; 1998.
[41] Brandrup J, Immergut EH. Polymer handbook. New York: Wiley; 1989.
[42] Kiran E, Xiong Y, Zhuang WH. J Supercrit Fluids 1993;6(4): 193–203.